Journal of Pharmaceutical Sciences 111 (2022) 1004–1011

Contents lists available at ScienceDirect

Journal of Pharmaceutical Sciences

journal homepage: www.jpharmsci.org

Special Topic Cluster

Tuning Surface Charges of Peptide Nanofibers for Induction of Antigen-Specific Immune Tolerance: An Introductory Study

Chun Yin Jerry Lau[a], Naomi Benne[b], Bo Lou[a,c], Daniëlle ter Braake[b], Esmeralda Bosman[a], Nicky van Kronenburg[a], Marcel H. Fens[a], Femke Broere[b], Wim E. Hennink[a], Enrico Mastrobattista[a,*]

[a] *Utrecht Institute for Pharmaceutical Sciences, Department of Pharmaceutics, Faculty of Science, Utrecht University, Universiteitsweg 99, 3584 CG Utrecht, the Netherlands*

[b] *Department of Infectious Diseases and Immunology, Faculty of Veterinary Medicine, Utrecht University, Yalelaan 1, 3584 CL Utrecht, the Netherlands*

[c] *Cardiovascular Research Institute, Department of Medicine, Yong Loo Lin School of Medicine, National University of Singapore, #08-01, MD6 Centre for Translational Medicine, 14 Medical Drive, 117599, Singapore*

ARTICLE INFO

Article history:
Received 5 December 2021
Revised 28 January 2022
Accepted 28 January 2022
Available online 1 February 2022

Keywords:
Peptides
Vaccines
Nanofibres
Aggregation
Immune tolerance

ABSTRACT

Induction of antigen-specific immune tolerance has emerged as the next frontier in treating autoimmune disorders, including atherosclerosis and graft-vs-host reactions during transplantation. Nanostructures are under investigation as a platform for the coordinated delivery of critical components, i.e., the antigen epitope combined with tolerogenic agents, to the target immune cells and subsequently induce tolerance. In the present study, the utility of supramolecular peptide nanofibers to induce antigen-specific immune tolerance was explored. To study the influence of surface charges of the nanofibers towards the extent of the induced immune response, the flanking charge residues at both ends of the amphipathic fibrillization peptide sequences were varied. Dexamethasone, an immunosuppressive glucocorticoid drug, and the ovalbumin-derived OVA323-339 peptide that binds to I-A(d) MHC Class II were covalently linked at either end of the peptide sequences. It was shown that the functional extensions did not alter the structural integrity of the supramolecular nanofibers. Furthermore, the surface charges of the nanofibers were modulated by the inclusion of charged residues. Dendritic cell culture assays suggested that nanofiber of less negative ζ-potential can augment the antigen-specific tolerogenic response. Our findings illustrate a molecular approach to calibrate the tolerogenic response induced by peptide nanofibers, which pave the way for better design of future tolerogenic immunotherapies.

Introduction

Autoimmune disorders (e.g., atherosclerosis and graft-vs-host reactions during transplantation) are rising in developed and rapidly developing countries.[1] There is currently no cure for autoimmune disorders. Standard treatments of autoimmune disorders involve symptom alleviation through pharmacological intervention. However, most immunosuppressive interventions are not targeted and affect the entire body, leading to undesirable systemic immunodeficiency and life-changing side effects. Therefore, to incur higher disease specificity towards immunosuppression, antigen-specific immunotolerance has emerged as the next frontier in autoimmune disorder treatments.[2-4]

The establishment of antigen-specific immune tolerance requires 1) surface presentation of disease-specific antigen epitopes on antigen-presenting cells (APCs); and 2) modulating APCs toward a tolerogenic phenotype, which leads to activation of antigen-specific regulatory T (Treg) cells. Nanoparticles are extensively explored as a platform for induction of antigen-specific immune tolerance, either through delivering antigen to APCs present in natural tolerogenic environments (e.g., liver),[5,6] or co-delivery of tolerogenic pharmacological agents (e.g., dexamethasone) and antigens to the APCs. In particular, the latter approach can steer the recipient APCs toward a tolerogenic phenotype, thereby avoiding the "off-target" induction of proinflammatory responses in the former approach[7-9] as well as limiting the side effects of long-term systemic immunosuppression, e.g.,

* Correspondence author.
E-mail address: e.mastrobattista@uu.nl (E. Mastrobattista).

https://doi.org/10.1016/j.xphs.2022.01.030

cancer promotion.[10] However, usage of conventional nanoparticles still encounters challenges in large-scale production[11] and stability and transport.[12,13]

Proteinaceous aggregates in the nano and microscale are known to display enhanced immune activity.[14,15] Harnessing this potential, several groups have engineered these proteinaceous aggregates for immunomodulatory applications.[16-18] In particular, β-sheet rich peptide nanofibers represent promising vaccination agents thanks to their multivalent functionality,[19,20] simple preparation procedure, and high thermal stability.[21,22] Furthermore, to avoid the unlimited growth of these β-sheet aggregates, the peptide can be molecularly engineered to regulate the assembly of these nanofibers (e.g., instigating molecular frustration).[31] Upon subcutaneous injection, these peptide nanofibers (<10nm in diameter, >200nm in length) can reach the site of action (lymphatic system) and elicit potent antigen-specific immune responses.[17,23] Moreover, unlike conventional vaccine adjuvants (e.g., colloidal alum), peptide nanofibers can induce antigen-specific immune responses without inducing local inflammation.[24] Like other nanoparticle-based vaccines,[25] the surface charge of peptide nanofibers is a pivotal parameter for adjusting their immunogenicity.[17] It was shown that reducing the negative charges on the nanofiber surfaces can augment the dendritic cell (DCs) uptake, leading to more robust immune responses. However, alteration of the nanofibers' surface charge alone was insufficient to establish antigen-specific immune tolerance.[17] Besides, control over nanofibers' aspect ratio (diameter and length) is another approach often employed for modulating the immune response.[16,26] Due to the inherent structural helicity, the width of peptide nanofibers is energetically restrained,[27,28] with a diameter generally between 3-10nm.[26,29,30] Regarding control over the length, Collier et al. showed that, in the range of 200-1800nm, shorter nanofibers could induce a more robust $CD8^+$ T cell response.[26] However, they also showed that length alteration of the nanofibers does not cause a significant effect on $CD4^+$ T cell responses. In this regard, Jiskoot et al. demonstrated that nanosized aggregates formed by adjuvant-antigen conjugates can efficiently control the resultant immune response.[18] Furthermore, they showed that these adjuvant-antigen aggregates can elicit more robust responses than the conventional antigen/adjuvant co-encapsulated nanoparticles. Therefore, it is hypothesized that ligation of tolerogenic adjuvants to peptide nanofibers presents a new opportunity in controlling the antigen-specific immune response.

This study investigated the effect of surface charge on the peptide nanofibers towards eliciting antigen-specific immunotolerance. Multidomain peptides (MDPs), a well-studied β-sheet forming sequence (-SLSLSLSLSLSL-) developed by Hartgerink et al., were deployed as the fibrillization domain.[31] Dexamethasone and the model ovalbumin (OVA) I-A(d) major histocompatibility complex (MHC) class II peptide epitope (OVA323-339: ISQAVHAAHAEINEAGR) were flanked at two ends of the fibrillization domain, spaced with either two positively charged lysine (K) or negatively charged glutamate (E) residues (Fig. 1a). The physicochemical properties of the peptide nanofibers' (morphology, ζ-potential, secondary structure) were subsequently characterized. Finally, the immune response elicited by nanofibers with different physicochemical properties was studied in murine bone marrow-derived dendritic cells (BMDC).

Materials and Methods

Materials

Pre-loaded Fmoc-Arg(Pbf)-Wang resin, Fmoc-protected amino acids were purchased from Novabiochem (Darmstadt, Germany). Oxyma pure was obtained from Manchester Organics (Manchester, UK). N, N'-Diisopropylcarbodiimide, acetonitrile (MeCN) was obtained from Biosolve BV (Valkenswaard, the Netherlands). Trifluoroacetic acid, triisopropylsilane, formic acid, ammonium

a

Peptide	Sequence
Dex-MDP-K-OVA323	Dexamethasone-succinyl spacer-KKSLSLSLSLSLSLKKISQAVHAAHAEINEAGR-COOH
Dex-MDP-E-OVA323	Dexamethasone-succinyl spacer-EESLSLSLSLSLSLEEISQAVHAAHAEINEAGR-COOH
Ac-MDP-K-OVA323	Ac-KKSLSLSLSLSLSLKKISQAVHAAHAEINEAGR-COOH
Ac-MDP-E-OVA323	Ac-EESLSLSLSLSLSLEEISQAVHAAHAEINEAGR-COOH

b

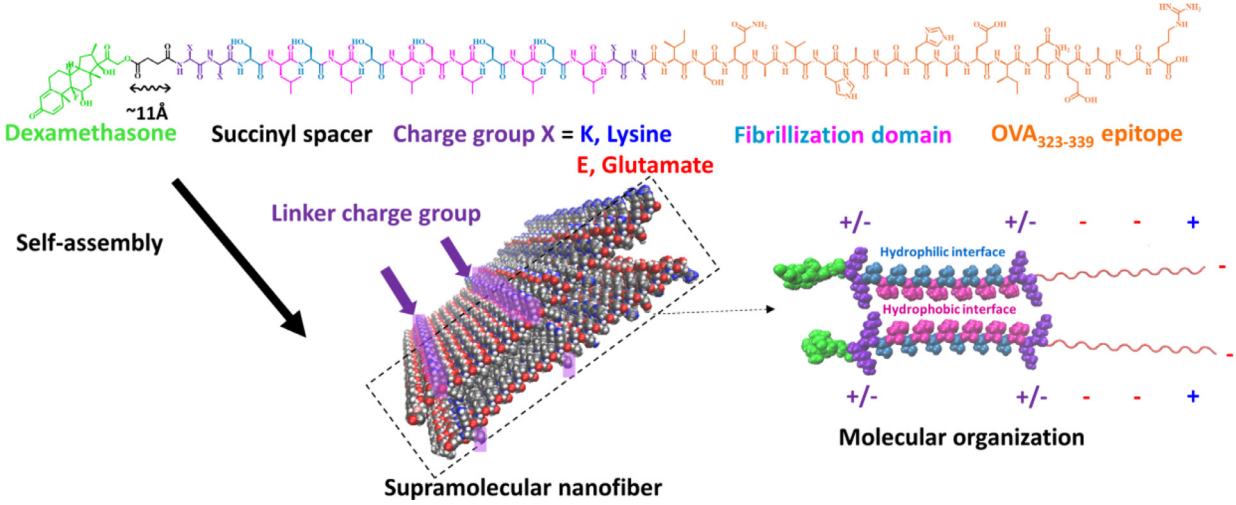

Fig. 1. Summary of peptides in this study and representation of the molecular arrangement in nanofibers. a) list of peptides studied in this work. b) Graphical representation of the molecular organization of the supramolecular nanofibers. The chemical structure of the multidomain (MDP) fibrillization domain consists of alternative arrangements of serine (hydrophilic, in blue) and leucine residues (hydrophobic residue, in magenta). This structural chemical anisotropy aids the molecular arrangement of nanofibers into hydrophilic and hydrophobic interfaces. Due to the arrangement of the nanofiber in the form of an anisotropic tape, the flanking charge groups are exposed at the nanofiber surface. All the surface exposed charged residues are marked with + or -.

bicarbonate, β-mercaptoethanol, and lipopolysaccharide were purchased from Sigma-Aldrich (Zwijndrecht, the Netherlands). Dulbecco's phosphate-buffered saline buffer (1 × PBS, 2.7mM KCl, 1.5mM KH2PO4, 138mM NaCl, 8mM Na2HPO4, pH 7.4), Roswell Park Memorial Institute Medium (RPMI 1640) medium, Iscove's Modified Dulbecco's Medium (IMDM), and penicillin/streptomycin were purchased from Lonza (Basel, Switzerland). Granulocyte-macrophage colony-stimulating factor (GM-CSF) was purchased from PeptroTech (London, UK). ViaKrome 808 Fixable Viability Dye (Cat# C36628) was purchased from Beckman Coulter (California, USA). Monoclonal antibodies specific for mouse CD4 (Cat# 11-0042-82), Foxp3 (Cat# 45-5773-82), and T-bet (Catalog # 17-5825-82) were purchased from eBioscience (California, USA), while the monoclonal antibodies specific for CD25 (Cat# 553866) was purchased from BD Bioscience (New Jersey, US). Fetal calf serum (FCS) was purchased from GE Healthcare (Little Chalfont, UK).

Synthesis and Preparation of the Supramolecular Peptide Nanofibers

Peptides (Fig. 1a) were synthesized in-house with standard Fmoc solid-phase chemistry using a Liberty blue peptide synthesizer (CEM Corporation, Matthews, US). Pre-loaded Fmoc-Arg(Pbf)-Wang resin was used as the starting material. For each coupling cycle, 5eq Fmoc-protected amino acids were activated with 5eq of Oxyma pure and N, N'-Diisopropylcarbodiimide to react with the free N-terminal amino acids in the resin for 1 minute at 90°C. After each coupling step, the Fmoc group was removed by treatment with 20% piperidine for 1 minute at 90°C. Dexamethasone succinate was synthesized as described before (Fig. 2a)[32] and conjugated to the free N-terminal of the protected peptide on the resin using the same coupling condition as with other Fmoc-amino acids (Fig. 2b). A cleavage cocktail, trifluoroacetic acid/water/triisopropylsilane (95/2.5/2.5), was used to simultaneously cleave the peptide off the resin and remove the side chain protecting groups. Crude products were purified by preparative reverse-phase HPLC using Reprosil-Pur C18 column (10 μm, 250 × 22 mm) eluted with water-MeCN gradient 5% to 80% MeCN (0.1% formic acid for K-containing peptides, 10mM ammonium bicarbonate for E-containing peptides) in 35 minutes at a flowrate of 15.0ml/min with UV detection at 220 nm. Purity was confirmed to be >90% by analytical HPLC-MS using Waters XBridge C18 column (5μm, 4.6 × 150 mm) eluted with water-MeCN gradient 5 to 80% MeCN (0.1% formic acid for K-containing peptides, 10mM ammonium bicarbonate for E-containing peptides) in 20 minutes at a flow rate 1.0 ml/min and UV detection at 220 nm. MS analysis was performed using a Bruker microTOF-Q instrument.

The nanofibers were prepared by dissolving peptides in sterile ultrapure water at a concentration of 8 mM. After overnight incubation at 4°C, the peptide solution was diluted to 2 mM in 1 × PBS buffer to reach pH value 7.3-7.5, followed by incubation at room temperature for 3 hours.[33]

Circular Dichroism (CD) & ζ-potential Measurement

The dispersions of nanofibers (2 mM in 1 × PBS) were diluted to 0.2 mM with 1 × PBS buffer for both CD and ζ -potential measurement. Far-UV CD spectra were recorded on a double beam DSM 1000 CD spectrometer (Online Instrument Systems, Athens, USA) from 260 to 180 nm in a quartz cuvette with 0.1 cm path length. Three accumulations were averaged for each sample, and the spectra were expressed in molar ellipticity (10^3 deg cm^2 dmol^{-1}). ζ-Potential was measured with a DTS1070 folded capillary cell on a Malvern Zetasizer Nano-Z (Malvern Instruments, Malvern, UK). Samples were equilibrated for 3 min at room temperature and measured 3 times, and results were shown as averaged.

Negative-staining Transmission Electron Microscopy (TEM)

The dispersions of nanofiber (2 mM) were diluted five-fold with 1X PBS buffer. Formvar/carbon-coated 400 mesh copper grids (Polysciences Inc., Warrington, US) were placed on top of a droplet of 20 μL of diluted samples. After 2 min incubation, the grid was washed three times with 0.2 μm filtered milli-Q water and blotted dry with filter paper. Negative staining was performed for 1 min with 2% w/v uranyl acetate in water. The staining solution was removed by blotting with filter paper. Samples were imaged on a Tecnai 20 microscope equipped with a 4 K square pixel Eagle CCD camera (FEI, Eindhoven, The Netherlands).

Mice

Eight weeks old female C57BL/6-Ly5.1 and C57BL/6-Tg(TcraTcrb) 425Cbn/Crl (OTII) mice were purchased from Charles River and kept under conventional conditions (type 3H filtertop Makrolon cages

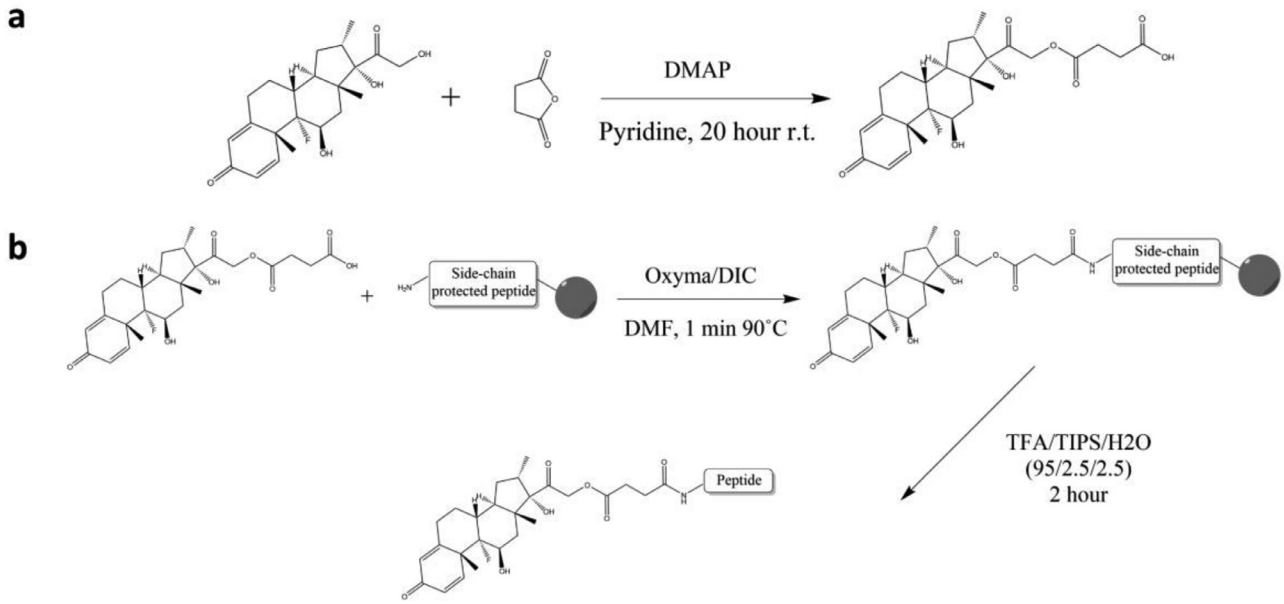

Fig. 2. Chemical synthesis pathway for a) dexamethasone succinate; b) dexamethasone-peptide conjugates.

(n=10/cage), type 2L filtertop Makrolon cages n=5/cage), respectively, (12h day/night cycles) at the animal facility. Mice were provided with tap water and food (SDS) ad libitum. All animal experiments were performed following the Dutch Animal Experimentation Act. EU directives 86/609/CEE and 2010/63/EU related to the protection of vertebrate animals used for experimental and other scientific purposes and were approved by the Committee on Animal Experiments of the University of Utrecht (DEC2015.II.811.050, 8 march 2016) and performed in the Central Laboratory Animal Research Facility of the University of Utrecht (GDL), which has AAALAC (Association for Assessment and Accreditation of Laboratory Animal Care) accreditation.

BMDCs

Bone marrow cells were isolated from the tibias and femurs of C57BL/6 mice, and a single-cell suspension was obtained using a 70 μm cell strainer (Greiner Bio-One B.V., Alphen aan den Rijn, the Netherlands). The bone marrow cells were seeded at 9×10^5 cells per well in a 6 well-plate and incubated for 7 days in IMDM medium supplemented with 2 mM glutamine, 10% FCS, 20 ng/mL GM-CSF, 100 U/mL penicillin/streptomycin, and 50 μM β-mercaptoethanol. The cells were cultured at 37 ℃. The medium was refreshed every other day. On day 7, cells were matured in the presence of 10 ng/mL lipopolysaccharide and used for the *In vitro* OVA-specific tolerogenic assay.

In vitro OVA-specific Tolerogenic Assay

The matured BMDCs were incubated with 10 μM of Dex-MDP-K/E-OVA, Ac-MDP-K/E-OVA nanofiber, or OVA323 epitope for 2 days. Afterward, CD4+ T cells were isolated from the spleens of OTII mice using a CD4+T cell isolation kit (Miltenyi Biotec B.V., Leiden, the Netherlands). The purified CD4+ T cells were added at a density of 1×10^5 cells per well and incubated for 3 days in a complete RPMI 1640 medium supplemented with 2 mM glutamine, 10% FCS, 100 U/mL penicillin/streptomycin, and 50 μM β-mercaptoethanol. The cells were stained for viability using ViaKrome 808 Fixable Viability Dye. Cells were further stained with monoclonal antibodies specific for mouse CD4, CD25, Foxp3, and T-bet. The proportion of Treg ($CD25^+Foxp3^+$) and T-helper 1 (Th-1, T-bet^+) cells in the live CD4+ T cell population was analyzed by flow cytometry using a Gallios flow cytometer (Beckman Coulter, California, US) and FlowJo 7.6.5 (Fig. S1).

Statistical Analysis

Statistical analysis was performed in GraphPad Prism v.9.1.1 using one-way ANOVA with Turkey's multiple comparison test. Data are presented as average± standard deviations unless otherwise indicated. Significant statistical difference is annotated as $^*p < 0.05$, $^{**}p < 0.01$, $^{***}p < 0.001$, $^{****}p < 0.0001$.

Results & Discussion

Molecular Design & Synthesis

To systematically investigate the effect of linker-charged residues on the formation of supramolecular nanofibers and antigen-specific tolerance induction, a library of MDPs with either K or E flanking residues appended to both ends of the fibrillization domain was designed (Fig. 1a). Via solid-phase chemistry (Fig. 2b), dexamethasone was conjugated to the N-terminus of the peptides via a biodegradable succinyl-spacer, which is susceptible to (intracellular) carboxylesterase degradation but is otherwise stable under physiological conditions.[32,34,35] The identities of the purified MDPs were confirmed using HPLC-MS (Fig. 3, Table 1). Since carboxylesterases are ubiquitously expressed in the intracellular compartment[36] and whole blood,[37,38] a short succinyl spacer (~11 Å extended length, Fig. 1b) was used to ensure the ester bond was inaccessible to the catalytic binding site of carboxylesterase in the nanofiber state, thereby preventing premature release of dexamethasone from the nanofiber before taking up by the APCs.[39] Once the APCs take up the nanofibers, the fibrous structure will be processed through autophagy.[40,41] Subsequently, the nanofibers are processed by aminopeptidase and

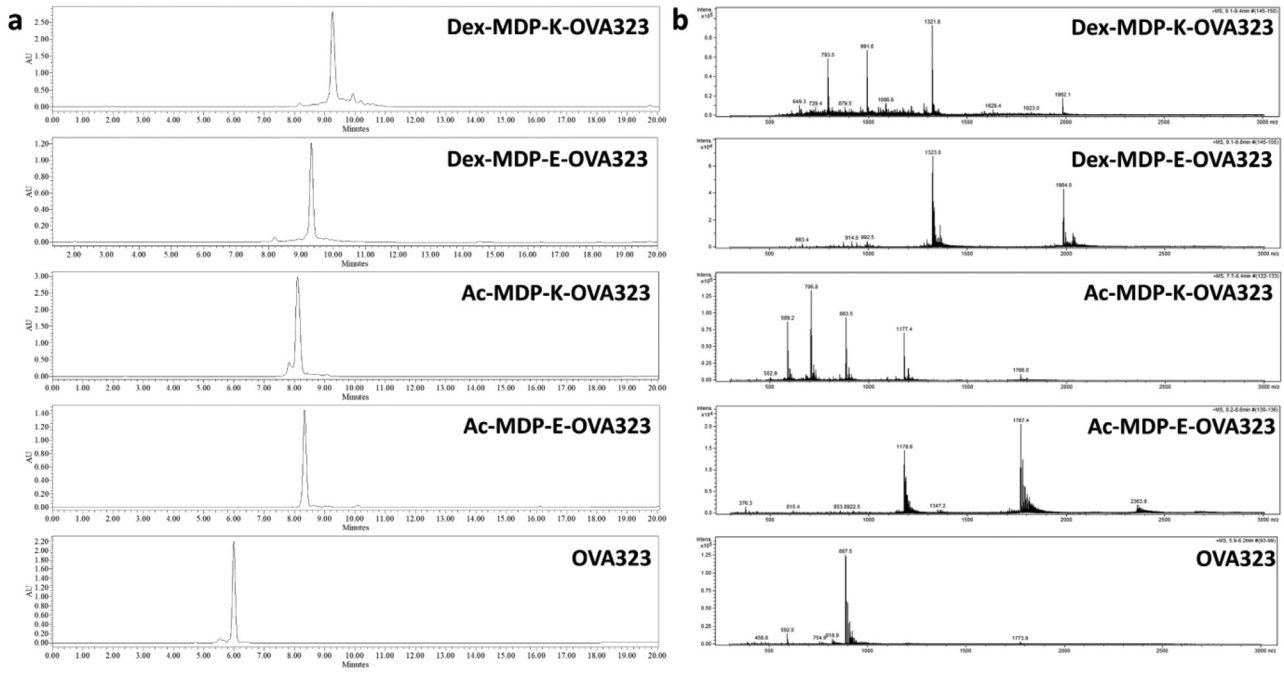

Fig. 3. Identify confirmation of the synthesized peptides. a) HPLC chromatograms of the synthesized peptides with a UV detection wavelength of 220nm; b) corresponding MS traces of the synthesized peptides

Table 1
Summary of the Theoretical Mass and the MS Trace Found.

Peptide	Theoretical Mass	Mass Found
Dex-MDP-K-OVA323	3962.6 Da	$[M+2H]^{2+}$=1982.3, [M+3H]3+=1321.9, [M+4H]4+=991.6, [M+5H] 5+=793.5
Dex-MDP-E-OVA323	3966.4 Da	$[M+2H]^{2+}$=1984.2, $[M+3H]^{3+}$=1323.1
Ac-MDP-K-OVA323	3530.1 Da	$[M+3H]^{3+}$=1177.7, [M+4H]4+=883.5, [M+5H]5+=707.0, [M+6H]6+=589.4
Ac-MDP-E-OVA323	3533.9 Da	$[M+2H]^{2+}$=1768.0, $[M+3H]^{3+}$=1179.0
OVA323	1173.9 Da	$[M+2H]^{2+}$=888.0

carboxylesterase, leading to antigen epitope processing and dexamethasone release to exert its antigen-specific tolerogenic effect.[4,10] To evaluate the effect of dexamethasone conjugation, two peptides composed of N-acetylated MDPs, Ac-MDP-K/E-OVA323 were included, for functional comparison with Dex-MDP-K/E-OVA323 (Fig. 1a).

Self-assembly & Physicochemical Characterization

The morphology of the peptide aggregates was characterized by transmission electron microscopy (TEM). TEM images confirm that peptide nanofibers were formed from all four MDP-containing peptides (~4nm diameter, >500nm long) (Fig. 4a). Even though Dex-MDP-K-OVA323 has the shortest range of nanofiber lengths among the 4 studied nanofibers (Figure S2), it was shown that these length differences have a negligible effect on the resultant CD4+ response.[26] Next, the mode of fibrillization of these peptides was investigated. Previous studies showed that the MDP sequence initiated fibrillization through the β-sheet formation. Using CD spectrometry, a single negative minimum at 220-230 nm and a positive band at 200-205 nm were observed in the different samples (Fig. 4b), which signifies that the β-sheet conformation is the predominant secondary structure in the investigated nanofiber systems.[17] Furthermore, amongst these 4 studied nanofibers, Dex-MDP-K-OVA323 has the most flattened minima at 220-230nm. It is plausible that amongst the 4 nanofibers studied, the supramolecular organization of the Dex-MDP-K-OVA323 nanofiber is the most favorable for the OVA323 sequence to maintain an α-helical conformation (Figure S3). Regarding the use of 1 × PBS as a buffer for ζ-potential measurement, the relatively high ionic strength and presence of multivalent ions (e.g., $HPO4^{2-}$) as compared to buffers of low ionic strength (e.g., 10-25 mM HEPES, pH 7.4) in which ζ-potential measurements are routinely measured can compress the electric double layer on the nanofiber surface, leading to a low ζ-potential value.[42] However, ζ-potential measurements in buffers of lower ionic strength can alter the nanofiber polymorphism, thereby changing the resultant surface chemistry.[43] Therefore, 1 × PBS was used to determine the ζ-potential of the nanofibers. Fig. 4c shows that the linker-charged residues influenced the ζ-potential of the peptide nanofibers. The K-containing nanofibers (Dex-/Ac-MDP-K-OVA323) exhibited less negative zeta potential (-2 to -4mV) when compared to the E-containing nanofibers (Dex-/Ac-MDP-E-OVA323, -20 to -23mV). This significant difference in ζ-potential can be explained by the inherent chemical anisotropy in the fibrillization domain, causing the MDP nanofibers to molecularly arrange in the form of an anisotropic tape[28] (Fig. 1b). Due to the molecular organization of the MDP nanofibers, the linker-charged residues are exposed at the surface of the nanofibers (highlighted in purple in Fig. 1b).

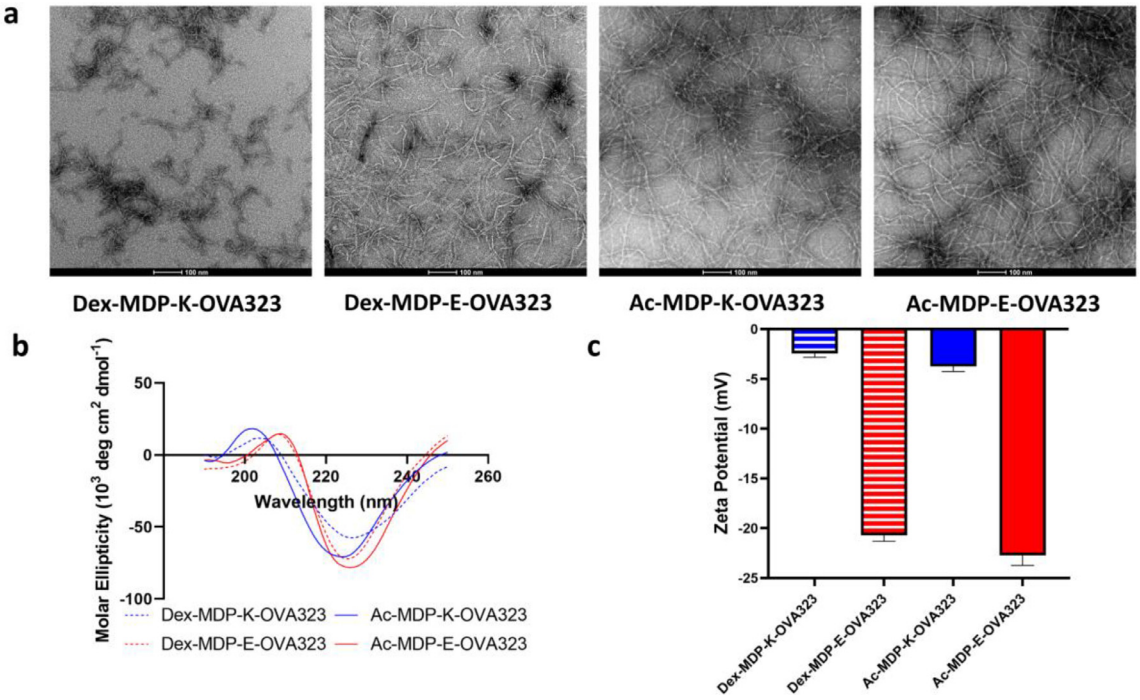

Fig. 4. Physicochemical properties of the formed peptide nanofibers. a) Negative-stain TEM images show that MDP nanofiber formation is not disturbed by conjugation of dexamethasone and/or OVA323 epitopes. b) CD spectra of the peptides studied. All peptides display signature β-sheet patterns (negative minima: 220-230nm; positive band: 200-205nm). This shows that the β-sheet is the driving force for the fibrillization process. c) ζ-potential of the peptide fibers studied. The K-containing nanofibers display a lower ζ-potential (-2 to -4mV), while the E-containing nanofibers display a more negative ζ-potential (-20 to -23mV). This shows that variation in charge of the flanking aa residues can alter the ζ-potential of the nanofibers. The ζ-potential Data expressed as the mean ± standard deviations

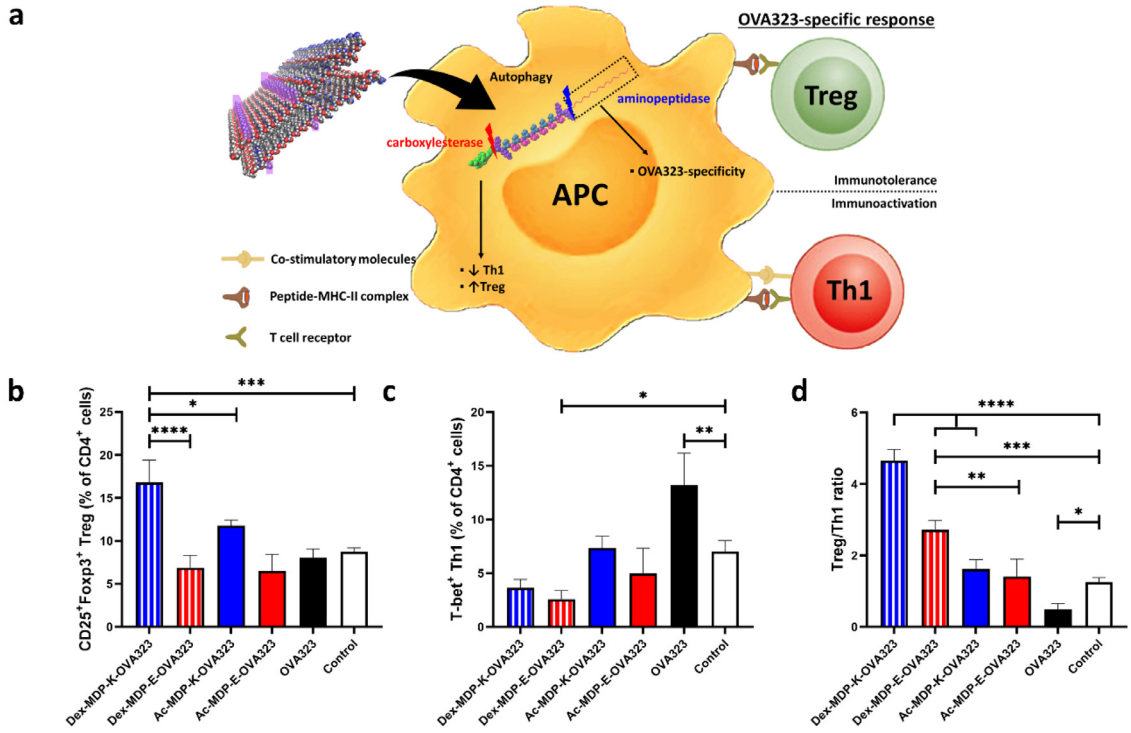

Fig. 5. *In vitro* tolerogenic effect of the nanofiber treatment. a) Graphical representation of the intracellular processing of the dexamethasone-containing nanofibers. The fibrous structure is first processed through autophagy engagement. Dexamethasone is then released by carboxylesterase catalyzed hydrolysis, which can upregulate regulatory T (Treg) level and lower the T helper 1 (Th1) level; while OVA323 epitope is processed by aminopeptidase to elicit antigen-specific response b,c) BMDCs were incubated with 10 μM of peptide nanofiber dispersions for 2 days. Subsequently, $CD4^+$ OTII T cells were added and incubated for 3 days. b) The level of Treg was analyzed by flow cytometry. Significant Treg expansion was only observed for Dex-MDP-K-OVA323 when compared to the negative control (PBS treatment). c) The level of Th1 was analyzed by flow cytometry. Dex-MDP-E-OVA323 treatment group significantly lowered the Th1 level compared to the negative control, while OVA323 treatment can significantly upregulate the Th1 level. d) The dexamethasone functionalized MDP nanofibers were both shown effective in establishing tolerogenic profiles (Treg/Th1 ratio), with Dex-MDP-K-OVA323 more effective than Dex-MDP-E-OVA323. Data were analyzed by one-way ANOVA with Turkey's multiple comparison test (compared to the OVA323 group) and expressed as the mean ± standard deviations (n=3); * $p < 0.05$, ** $p < 0.01$, *** $p < 0.001$, **** $p < 0.0001$.

Dex-MDP-K-OVA323 Upregulated OVA323-specific Treg

To investigate whether Dex-MDP-OVA323 nanofibers can induce antigen-specific Tregs, BMDCs were incubated with the nanofibers for 2 days, followed by 3 days of co-culturing with $CD4^+$ T cells freshly isolated from the spleens of OTII mice. The level of OVA323-specific immune tolerance was probed by the relative amount of Treg cells compared to all $CD4^+$ T cells. BMDC that received 1XPBS was included as sham treatment throughout the *in vitro* tolerogenic assay. It was observed that only the Dex-MDP-K-OVA323 nanofiber formulation significantly expanded the Treg level amongst all the treatment groups (Fig. 5b). The differential Treg induction effect between Dex-MDP-K-OVA323 and Ac-MDP-K-OVA323 shows that dexamethasone functionalization is essential for establishing antigen-specific immune tolerance (Fig. 5b). The failure for Ac-MDP-K/E-OVA323 to expand Treg concur with the previous findings that variation in the nanofiber surface charge alone was insufficient to establish immune tolerance.[17] Finally, the difference in Treg induction between Dex-MDP-K-OVA323 and Dex-MDP-E-OVA323 show that reducing the surface negative charges can potentiate the induction of Treg. The difference in Treg level is likely caused by the higher uptake of the nanofibers by the DCs due to the lower electrostatic repulsion between the negatively charged cell surface and nanofibers.[17]

Dex-MDP-E-OVA323 Downregulated OVA323-specific Th-1

Since parallel activation of proinflammatory effector T cells is undesirable for the potential treatment of autoimmune disorders,[44-46] the level of antigen-specific Th1 cells was monitored to validate the balance of the immune response. The autoreactive Th1 cell level was chosen for monitoring as its upregulation can exacerbate autoimmune disorders such asatherosclerosis[44,45] or diabetic coronary artery disease.[46] It was observed that all MDP nanofiber treatment groups did not upregulate the Th1 level (Fig. 5c). The absence of autoreactive Th1 activation by the MDP nanofiber treatment groups concurred with the previous observations about the ability of nanofibers to serve as a non-inflammatory vaccine adjuvant.[24] Furthermore, a significant downregulation of Th1 cells was observed for the Dex-MDP-E-OVA323 treatment group. This shows that, despite failing to upregulate OVA323-specific Treg, Dex-MDP-E-OVA323 can exert its tolerogenic effect by tuning down the OVA323-specific Th-1 level (Fig. 5c). Besides, treatment of the OVA323 epitope alone has been shown to upregulate the Th1 level significantly. This shows that the matured BMDCs displayed an immunogenic phenotype under the above-specified culture conditions (especially the seeding density).[47] Therefore, it illustrates that the BMDC model can serve as a relevant model in assaying the ability of the MDP nanofibers to reverse the immunogenic phenotype of DCs.

Dex-MDP-K-OVA323 More Efficient than Dex-MDP-E-OVA323 in Establishing Tolerogenic Profiles (Treg/Th1)

Finally, since Treg and Th1 are reciprocally regulated in the body,[48,49] the ratio between Treg and Th1 (Treg/Th1) can indicate the overall tolerogenic effect induced by the MDP nanofibers. Dexamethasone functionalized MDP nanofibers can steer antigen-specific tolerance, while the unfunctionalized MDP nanofibers failed to do so (Fig. 5d). Furthermore, Dex-MDP-K-OVA323 can elicit a more potent tolerogenic effect than Dex-MDP-E-OVA323 (Fig. 5d). Taken together, these results show that dexamethasone-incorporated nanofibers are

capable of inducing antigen-specific immune tolerance without parallel proinflammatory immune activation. Furthermore, it shows that, like other particulate vaccines, the surface property of the peptide nanofibers is critical parameters governing the immune response[25] and the extent of immune tolerance is increased by lowering the negative ζ-potential of the peptide nanofibers.

Conclusion

In summary, the application of dexamethasone-incorporated peptide nanofibers for the induction of antigen-specific immune tolerance was explored. It was shown that the supramolecular organization of the nanofibers remained unaltered amid functional extension. Further, the incorporation of anionic or cationic amino acid residues at each end of the fibrillization domain was shown to be an effective approach in changing the ζ-potential of the nanofibers. The extent of the tolerogenic response was found to be influenced by the ζ-potential of the nanofibers. Nanofibers with less negative ζ-potential gave a more robust tolerogenic response in the BMDC model. Our study offers a molecular approach to calibrate the magnitude (*i.e.*, Treg/Th1 ratio) and the type (*i.e.*, Treg or Th1 level) of tolerogenic response induced by peptide nanofibers. This knowledge paves the way for better design of future tolerogenic immunotherapies, such as antigen-specific Treg cell-based therapy[50] or *in vivo* application for eliciting *in-situ* tolerogenic response.[6,51] Further studies are needed to investigate how these modifications can affect nanofibers interaction with the biological environment (e.g., opsonisation, albumin binding), which also plays a critical role towards the immunological outcomes.

Author Contributions

Chun Yin Jerry Lau: Conceptualization, Data curation, Formal analysis, Investigation, Methodology, Project administration, Visualization, Writing - original draft, Writing - review & editingNaomi Benne: Data curation, Formal analysis, Methodology, ResourcesBo Lou: Data curation, Formal analysisDaniëlle ter Braake: Data curation, Formal analysisEsmeralda Bosman: Data curation, Formal analysisNicky van Kronenburg: Data curation, Formal analysisMarcel H. Fens: Data curation, Formal analysisFemke Broere: Data curation, Formal analysis, Methodology, ResourcesWim E. Hennink: Conceptualization, Funding acquisition, Methodology, Project administration, Resources, Supervision, Validation, Writing - review & editing.Enrico Mastrobattista: Conceptualization, Funding acquisition, Investigation, Methodology, Project administration, Resources, Supervision, Validation, Writing - original draft, Writing - review & editing.

Declaration of Interests

The authors declare that they have no known competing financial interests or personal relationships that could have appeared to influence the work reported in this paper.

Acknowledgement

C.Y.J.L acknowledges the support from the European Union (Horizon 2020 NANOMED Grant 676137).

Supplementary Materials

Supplementary material associated with this article can be found in the online version at doi:10.1016/j.xphs.2022.01.030.

References

1. Laayouni H, Oosting M, Luisi P, et al. Convergent evolution in European and Rroma populations reveals pressure exerted by plague on Toll-like receptors. Proc Natl Acad Sci. 2014;111(7):2668.
2. Sakaguchi S, Miyara M, Costantino CM, Hafler DA. FOXP3+ regulatory T cells in the human immune system. Nat Rev Immunol. 2010;10(7):490–500.
3. Pishesha N, Harmand T, Smeding LY, et al. Induction of antigen-specific tolerance by nanobody–antigen adducts that target class-II major histocompatibility complexes. Nat Biomed Eng. 2021.
4. Pickens CJ, Christopher MA, Leon MA, et al. Antigen-drug conjugates as a novel therapeutic class for the treatment of antigen-specific autoimmune disorders. Mol Pharmaceutics. 2019;16(6):2452–2461.
5. Pearson RM, Casey LM, Hughes KR, Miller SD, Shea LD. In vivo reprogramming of immune cells: technologies for induction of antigen-specific tolerance. Adv Drug Deliv Rev. 2017;114:240–255.
6. Liu Q, Wang X, Liu X, et al. Use of polymeric nanoparticle platform targeting the liver to induce Treg-mediated antigen-specific immune tolerance in a pulmonary allergen sensitization model. *ACS Nano*. 2019;13(4):4778–4794.
7. Kishimoto TK, Maldonado RA. Nanoparticles for the induction of antigen-specific immunological tolerance. Front Immunol. 2018;9:230.
8. Kim S-H, Moon J-H, Jeong S-U, Lee C-K. Induction of antigen-specific immune suppression using biodegradable nanoparticles containing antigen and dexamethasone. J Immunol. 2019;202(1 Supplement): 177.3.
9. Liu Q, Wang X, Liu X, et al. Antigen- and epitope-delivering nanoparticles targeting liver induce comparable immunotolerance in allergic airway disease and anaphylaxis as nanoparticle-delivering pharmaceuticals. *ACS Nano*. 2021;15(1):1608–1626.
10. Sands RW, Tabansky I, Verbeke CS, et al. Steroid–peptide immunoconjugates for attenuating T cell responses in an experimental autoimmune encephalomyelitis murine model of multiple sclerosis. Bioconjugate Chem. 2020;31(12):2779–2788.
11. Bresseleers J, Bagheri M, Storm G, et al. Scale-up of the manufacturing process to produce docetaxel-loaded mPEG-b-p(HPMA-Bz) block copolymer micelles for pharmaceutical applications. Org Process Res Dev. 2019;23(12):2707–2715.
12. Ojha T, Hu Q, Colombo C, et al. Lyophilization stabilizes clinical-stage core-cross-linked polymeric micelles to overcome cold chain supply challenges. Biotechnol J. 2021;16(6):2000212.
13. Crommelin DJA, Anchordoquy TJ, Volkin DB, Jiskoot W, Mastrobattista E. Addressing the cold reality of mRNA vaccine stability. J Pharm Sci. 2021;110(3):997–1001.
14. Kijanka G, Bee JS, Bishop SM, Que I, Löwik C, Jiskoot W. Fate of multimeric oligomers, submicron, and micron size aggregates of monoclonal antibodies upon subcutaneous injection in mice. J Pharm Sci. 2016;105(5):1693–1704.
15. Ahmadi M, Bryson CJ, Cloake EA, et al. Small amounts of sub-visible aggregates enhance the immunogenic potential of monoclonal antibody therapeutics. Pharm Res. 2015;32(4):1383–1394.
16. Hainline KM, Fries CN, Collier JH. Progress toward the clinical translation of bioinspired peptide and protein assemblies. Adv Healthc Mater. 2018;7(5):1700930.
17. Wen Y, Waltman A, Han H, Collier JH. Switching the immunogenicity of peptide assemblies using surface properties. *ACS Nano*. 2016;10(10):9274–9286.
18. Slütter B, Bal SM, Que I, et al. Antigen–adjuvant nanoconjugates for nasal vaccination: an improvement over the use of nanoparticles? Mol Pharm. 2010;7(6):2207–2215.
19. Pompano RR, Chen J, Verbus EA. Titrating T-cell epitopes within self-assembled vaccines optimizes CD4+ helper T cell and antibody outputs. Adv Healthc Mater. 2014;3(11):1898–1908.
20. Shores LS, Kelly SH, Hainline KM, Suwanpradid J, MacLeod AS, Collier JH. Multifactorial design of a supramolecular peptide anti-IL-17 vaccine toward the treatment of psoriasis. Front Immunol. 2020;11:1855.
21. Sun T, Han H, Hudalla GA, Wen Y, Pompano RR, Collier JH. Thermal stability of self-assembled peptide vaccine materials. Acta Biomater. 2016;30:62–71.
22. Kelly SH, Opolot EE, Wu Y, Cossette B, Varadhan AK, Collier JH. Tabletized supramolecular assemblies for sublingual peptide immunization. Adv Healthc Mater. 2021 2001614. *n/a* (n/a).
23. Rudra JS, Tian YF, Jung JP, Collier JH. A self-assembling peptide acting as an immune adjuvant. Proc Nat Acad Sci USA. 2010;107(2):622–627.
24. Chen J, Pompano RR, Santiago FW, et al. The use of self-adjuvanting nanofiber vaccines to elicit high-affinity B cell responses to peptide antigens without inflammation. Biomaterials . 2013;34(34):8776–8785.
25. Benne N, van Duijn J, Kuiper J, Jiskoot W, Slütter B. Orchestrating immune responses: How size, shape and rigidity affect the immunogenicity of particulate vaccines. J Controll Rel. 2016;234:124–134.
26. Fries CN, Wu Y, Kelly SH, et al. Controlled lengthwise assembly of helical peptide nanofibers to modulate CD8+ T-cell responses. Adv Mater. 2020;32(39):2003310.
27. Aggeli A, Nyrkova IA, Bell M, et al. Hierarchical self-assembly of chiral rod-like molecules as a model for peptide β-sheet tapes, ribbons, fibrils, and fibers. Proc Natl Acad Sci. 2001;98(21):11857.
28. Hall DM, Bruss IR, Barone JR, Grason GM. Morphology selection via geometric frustration in chiral filament bundles. Nat Mater. 2016;15(7):727–732.
29. Fitzpatrick AWP, Debelouchina GT, et al. Atomic structure and hierarchical assembly of a cross-β amyloid fibril. Proc Natl Acad Sci. 2013;110(14):5468.
30. Lau CYJ, Fontana F, Mandemaker LDB, et al. Control over the fibrillization yield by varying the oligomeric nucleation propensities of self-assembling peptides. Commun Chem. 2020;3(1):164.

31. Lopez-Silva TL, Leach DG, Azares A, Li IC, Woodside DG, Hartgerink JD. Chemical functionality of multidomain peptide hydrogels governs early host immune response. Biomaterials . 2020;231:119667.
32. Acedo M, Tarrason G, Piulats J, Mann M, Wilm M, Eritja R. Preparation of oligonucleotide-dexamethasone conjugates. Bioorg Med Chem Lett. 1995;5(15):1577–1580.
33. Leach DG, Dharmaraj N, Piotrowski SL, et al. STINGel: controlled release of a cyclic dinucleotide for enhanced cancer immunotherapy. Biomaterials . 2018;163:67–75.
34. Li J, Kuang Y, Shi J, et al. Enzyme-instructed intracellular molecular self-assembly to boost activity of cisplatin against drug-resistant ovarian cancer cells. Angew Chem Int Ed. 2015;54(45):13307–13311.
35. Tang W, Zhao Z, Chong Y, et al. Tandem enzymatic self-assembly and slow release of dexamethasone enhances its antihepatic fibrosis effect. *ACS Nano*. 2018;12(10):9966–9973.
36. Hatfield JM, Wierdl M, Wadkins RM, Potter PM. Modifications of human carboxylesterase for improved prodrug activation. Expert Opin Drug Metab Toxicol. 2008;4(9):1153–1165.
37. Kalicharan RW, Bout MR, Oussoren C, Vromans H. Where does hydrolysis of nandrolone decanoate occur in the human body after release from an oil depot? Int J Pharm. 2016;515(1):721–728.
38. Kalicharan RW, Oussoren C, Schot P, de Rijk E, Vromans H. The contribution of the in-vivo fate of an oil depot to drug absorption. Int J Pharm. 2017;528(1):595–601.
39. Conda-Sheridan M, Lee SS, Preslar AT, Stupp SI. Esterase-activated release of naproxen from supramolecular nanofibres. Chem Commun. 2014;50(89):13757–13760.
40. Rudra JS, Khan A, Clover TM, et al. Supramolecular peptide nanofibers engage mechanisms of autophagy in antigen-presenting cells. *ACS Omega*. 2017;2(12):9136–9143.
41. Kaganovich D, Kopito R, Frydman J. Misfolded proteins partition between two distinct quality control compartments. Nature . 2008;454:1088.
42. Bhattacharjee S. DLS and zeta potential – What they are and what they are not? J Controll Rel. 2016;235:337–351.
43. Seuring C, Verasdonck J, Ringler P, et al. Amyloid fibril polymorphism: almost identical on the atomic level, mesoscopically very different. J Phys Chem B. 2017;121(8):1783–1792.
44. Hansson GK, Nilsson J. Developing a vaccine against atherosclerosis. Nat Rev Cardiol. 2020;17(8):451–452.
45. Tracy RP, Doyle MF, Olson NC, et al. T-helper Type 1 bias in healthy people is associated with cytomegalovirus serology and atherosclerosis: the multi-ethnic study of atherosclerosis. J Am Heart Assoc. 2022;2(3):e000117.
46. Madhumitha H, Mohan V, Deepa M, Babu S, Aravindhan V. Increased Th1 and suppressed Th2 serum cytokine levels in subjects with diabetic coronary artery disease. Cardiovasc Diabetol. 2014;13(1):1.
47. Nasi A, Bollampalli VP, Sun M, et al. Immunogenicity is preferentially induced in sparse dendritic cell cultures. Sci Rep. 2017;7(1):43989.
48. Klysz D, Tai X, Robert Philippe A, et al. Glutamine-dependent α-ketoglutarate production regulates the balance between T helper 1 cell and regulatory T cell generation. Sci Signal. 2015;8(396):ra97.
49. Liu G, Yang K, Burns S, Shrestha S, Chi H. The S1P1-mTOR axis directs the reciprocal differentiation of TH1 and Treg cells. Nat Immunol. 2010;11(11):1047–1056.
50. Raffin C, Vo LT, Bluestone JA. Treg cell-based therapies: challenges and perspectives. Nat Rev Immunol. 2020;20(3):158–172.
51. Maldonado RA, LaMothe RA, Ferrari JD, et al. Polymeric synthetic nanoparticles for the induction of antigen-specific immunological tolerance. Proc Natl Acad Sci. 2015;112(2):E156.